

Effects of metallic spacer in layered superconducting $\text{Sr}_2(\text{Mg}_y\text{Ti}_{1-y})\text{O}_3\text{FeAs}$

Kwan-Woo Lee

Received: date / Accepted: date

Abstract The highly two-dimensional superconducting system $\text{Sr}_2(\text{Mg}_y\text{Ti}_{1-y})\text{O}_3\text{FeAs}$, recently synthesized in the range of $0.2 \leq y \leq 0.5$, shows an Mg concentration-dependent T_c . Reducing the Mg concentration from $y=0.5$ leads to a sudden increase in T_c , with a maximum $T_c \approx 40$ K at $y=0.2$. Using first principles calculations, the unsynthesized stoichiometric $y=0$ and the substoichiometric $y=0.5$ compounds have been investigated. For the 50% Mg-doped phase ($y=0.5$), $\text{Sr}_2(\text{Mg}_y\text{Ti}_{1-y})\text{O}_3$ layers are completely insulating spacers between FeAs layers, leading to the fermiology such as that found for other Fe pnictides. At $y=0$, representing a phase with metallic Sr_2TiO_3 layers, the Γ -centered Fe-derived Fermi surfaces (FSs) considerably shrink or disappear. Instead, three Γ -centered Ti FSs appear, and in particular two of them have similar size, like in MgB_2 . Interestingly, FSs have very low Fermi velocity in large fractions: the lowest being 0.6×10^6 cm/s. Furthermore, our fixed spin moment calculations suggest the possibility of magnetic ordering, with magnetic Ti and nearly nonmagnetic Fe ions. These results indicate a crucial role of $\text{Sr}_2(\text{Mg}_y\text{Ti}_{1-y})\text{O}_3$ layers in this superconductivity.

Keywords Superconductivity · Fe-pnictides · Electronic Structure · Fermiology

1 Introduction

Since Hosono and coworkers discovered superconductivity in hole-doped LaFeAsO at $T_c=26$ K,[1] Fe-pnictides

have been the cause of much excitement.[2] The mechanism of the superconductivity has yet to be uncovered, but many have discussed the nesting of two Fermi surfaces at the Γ and M points.[3,4,5,6] However, some experimental and theoretical investigations of a few superconducting Fe-pnictides have shown the absence of a nested fermiology, though these compounds are expected to share a common mechanism of the superconductivity. [7,8,9,10]

In the pnictide family, the recently synthesized 21322 systems $\text{Sr}_2\text{MO}_3\text{FePn}$ (\mathcal{M} =transition metal, and $\text{Pn}=\text{P}$ or As), with a thick perovskite-like spacer between FePn layers, have stimulated a great enthusiasm due to its possible bimetallic character as well as its high two-dimensionality.[11,12,13,14,15,16] Sato *et al.* synthesized a member of the 21311 system $\text{Sr}_2(\text{Mg}_y\text{Ti}_{1-y})\text{O}_3\text{FeAs}$ in the range of $0.2 \leq y \leq 0.5$. [13] With 50% Mg doping of the Ti sites (*i.e.*, $y=0.5$), the superconductivity appears at $T_c=10$ K, but with a small superconducting volume fraction, which thus implies that there is no intrinsic superconductivity. On reducing the Mg concentration, T_c increases sharply to ~ 34 K at $y=0.45$, and reaches a maximum ~ 40 K at $y=0.2$, slightly higher than that in a stoichiometric $\text{Sr}_2\text{VO}_3\text{FeAs}$. Throughout all of the doping range considered, no significant changes in the lattice constants were observed. Although synthesis of a sample below $y=0.2$ has not been successful yet, the Ti rich phase may be expected to have a higher T_c . This implies that the Ti ions play a crucial role in the superconductivity of this system.

From the viewpoint of formal charge, the $y=0.5$ phase (*i.e.*, 50% Mg doping) consists of tetravalent Ti ions of d^0 , leading to a wholly insulating block between FeAs layers. Replacing a fraction of the sites containing Mg ions with Ti ions, Ti^{4+} ion becomes metallic $d^{1-2y} \text{Ti}^{(3+2y)+}$ on the average. Thus, this system is a

K.-W. Lee

Department of Display and Semiconductor Physics, Korea University, Sejong 339-700, Korea

Department of Applied Physics, Graduate School, Korea University, Sejong 339-700, Korea

E-mail: mckwan@korea.ac.kr

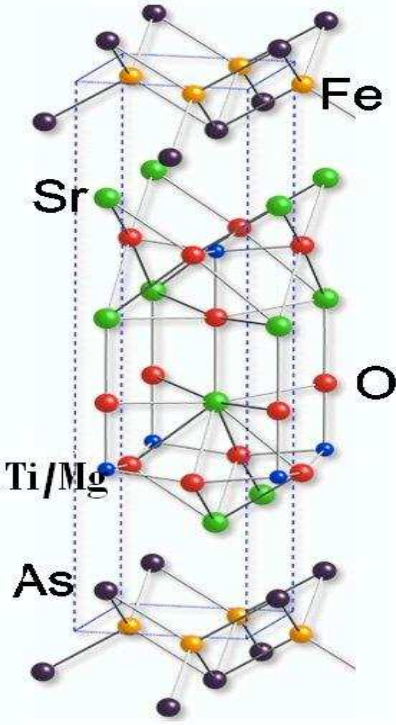


Fig. 1 Crystal structure of $\text{Sr}_2(\text{Mg}_y\text{Ti}_{1-y})\text{O}_3\text{FeAs}$, in which FeAs layers are separated by two Sr_2MO_3 blocks. The Fe-As bond length is 2.32 Å.

good example for investigating the effects of metallic and insulating spacers on the superconductivity. The effects of a metallic spacer have been under debate for $\text{Sr}_2\text{VO}_3\text{FeAs}$ having V (d^2) layers.[7,17]

In this paper, we investigate the $y=0.5$ and 0 phases, which represent either pure insulating or metallic spacers, respectively. So far, no evidence of magnetic ordering has been reported in this compound. We therefore will focus on the electronic structures and Fermi surfaces of the nonmagnetic (NM) state, though possible magnetic tendencies will also be discussed briefly.

2 Structure and Calculation Method

In our calculations, based on the tetragonal unit cell with $P4/nmm$ space group, the experimentally measured lattice constants $a=3.935$ Å and $c=15.952$ Å were used, resulting in a slightly larger volume by 2% than in $\text{Sr}_2\text{VO}_3\text{FeAs}$. [13] In the cell, Fe atoms lie at $2a$ sites $(\frac{1}{4}, \frac{3}{4}, 0)$, Ti/Mg, Sr, As, and O atoms lie at $2c$ sites $(\frac{1}{4}, \frac{3}{4}, z)$, and another O atoms sit at the $4f$ sites $(\frac{1}{4}, \frac{3}{4}, z)$. Using the local density approximation (LDA), the internal parameters were optimized to 0.3072 for Ti, 0.8210 and 0.5898 for two Sr sites, 0.0772 for As, 0.4270 for O at $2c$ sites, and 0.2939 for O at $4f$ sites. These values

lead to the As-Fe-As bond angle of $\alpha=116^\circ$, which is measured in one side of the Fe layer, corresponding to $T_c \approx 25$ K in the literature.[18] This significant difference from $T_c \approx 40$ K suggests a crucial role of the Sr_2MO_3 layer. The Mg-rich phase $\text{Sr}_2\text{Ti}_{\frac{1}{2}}\text{Mg}_{\frac{1}{2}}\text{O}_3\text{FeAs}$ was understood with a 2×1 supercell using our optimized internal parameters. In these optimization processes, the residual Hellman-Feynman forces on the atoms were lower than 1 meV/Å.

In all calculations, the local spin density approximation (LSDA) implemented in the accurate all-electron full-potential local orbital code, FPLO, was used.[19] A regular mesh containing 196 k points in the irreducible wedge was used to sample the Brillouin zone. The magnetic tendencies in the $y=0$ phase were studied using the fixed spin moment (FSM) method,[20] with a much denser mesh of up to 726 irreducible k points.

3 Results

3.1 50% Mg doped phase: $\text{Sr}_2\text{Ti}_{\frac{1}{2}}\text{Mg}_{\frac{1}{2}}\text{O}_3\text{FeAs}$

First, we will address the electronic structure of the $y=0.5$ phase having the insulating spacer. Figure 2 displays the enlarged band structure with the fatband of the Ti t_{2g} manifold (top panel) and the fatband of the Fe d manifold (bottom panel). Note that the X and M points in the unit cell are folded into the Γ and X points in the 2×1 supercell, respectively. The corresponding DOS near the Fermi energy E_F is given in Fig. 3. As expected, in the $y=0.5$ phase, the $3d$ orbitals of the Ti ions are completely unoccupied. The Ti t_{2g} manifold expands from 0.5 eV to 2 eV. In this phase, the details near E_F are very similar to those observed for other superconducting Fe-pnictides.[21,22,23,24] At the Γ point, three hole pockets derived from the Fe $d_{x^2-y^2}$, d_{yz} , and d_{zx} bands appear, while two-fold M -centered electron pockets with the character of these three bands also appear. Considering that there is no intrinsic superconductivity at this phase and the similar fermiology with other superconducting Fe pnictides, the nesting effects may not be a necessary ingredient for Fe pnictides to be superconductors.

3.2 Electronic structure of nonmagnetic $y=0$ phase

Now, we will focus on the $y=0$ phase, which contains only the metallic d^1 Ti^{3+} ions. Thus, this represents the phase of the range of $0 \leq y < 0.5$, consisting of metallic spacers. In this subsection, we will address the electronic structure of the NM state. The enlarged band

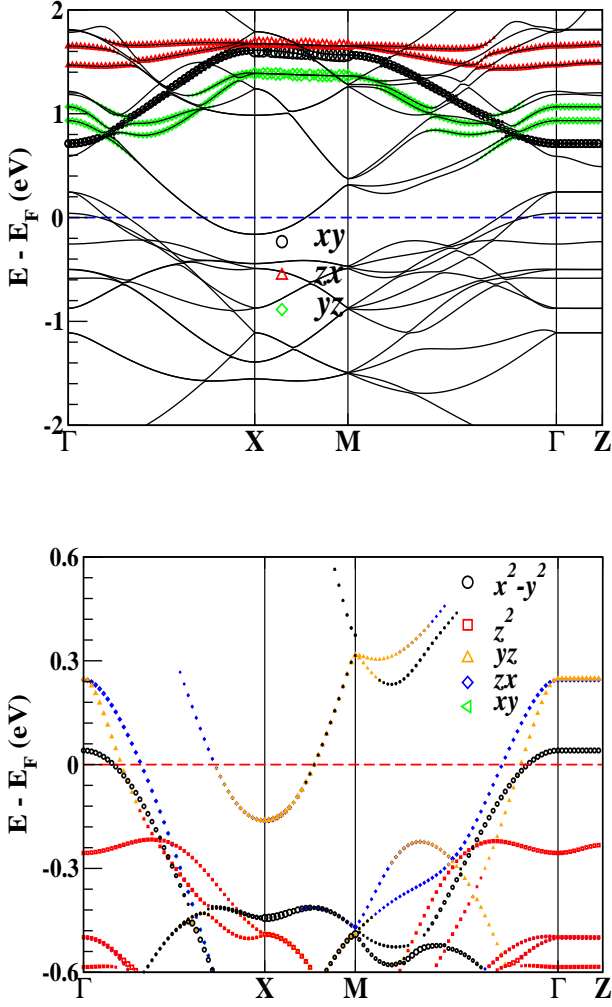


Fig. 2 Top: Band structure, with the fatband of Ti t_{2g} manifold, of nonmagnetic $2(\text{Sr}_2\text{Ti}_{\frac{1}{2}}\text{Mg}_{\frac{1}{2}}\text{O}_3\text{FeAs})$ in the 2×1 supercell. The Ti d_{zx} band lying around 1.8 eV is nearly dispersionless and separated from the Ti d_{yz} band. Bottom: Enlarged fatband representation of Fe d bands near the Fermi energy E_F , which is set to zero. The character of Fe d_{xy} band appears in the range of -2.2 to -1.1 eV and 0.6 to 1.6 eV (not shown here). In the fatband representation, the size of the symbols is proportional to the fractional character of each orbital.

structure near E_F and the fatband of the Ti t_{2g} manifold are displayed in the top panel of Fig. 4. The incomplete TiO_5As octahedron results in a breaking of the symmetry of the t_{2g} manifold. The partially filled Ti d_{xy} band spreads over the range of -0.7 to 1.6 eV (here, E_F is set to zero), which is a width that is 15% larger than that of the V d_{xy} band in $\text{Sr}_2\text{VO}_3\text{FeAs}$.^[7] This band can be described by a single-band tight-binding model with nearest neighbor hopping of $t=0.28$ eV and next neighbor hopping of $t'=0.08$ eV, *i.e.*, values that are about 15% larger than in $\text{Sr}_2\text{VO}_3\text{FeAs}$.^[7] The other

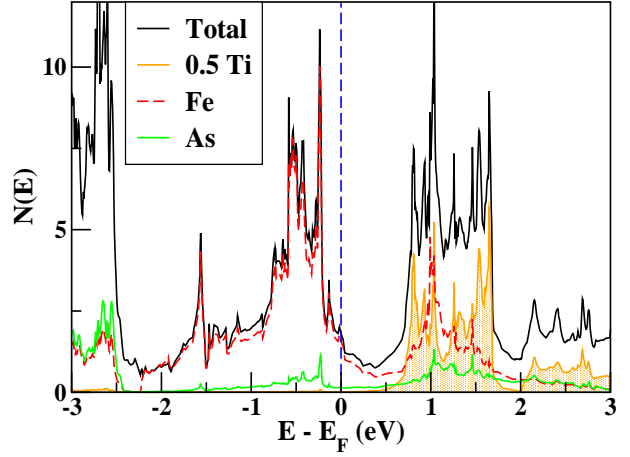


Fig. 3 Total and atom-projected densities of states (DOSs) on nonmagnetic $\text{Sr}_2\text{Ti}_{\frac{1}{2}}\text{Mg}_{\frac{1}{2}}\text{O}_3\text{FeAs}$ in the 2×1 supercell. DOS at E_F $N(E_F)$ is 1.82 states per eV per formula unit, 30% smaller than the value in LaFeAsO .^[21]

bands of Ti are mostly unoccupied, but there is some E_F crossing in the d_{yz} and d_{zx} bands near the Γ point, as shown in the bottom panel of Fig. 4. Although the hybridization of FeAs layers and the intervening Ti layers is negligible in almost the whole regime due to high two-dimensionality, small mixing with Fe d_{zx} and d_{yz} leads to this E_F crossing (see below).

Compared with other superconducting Fe-pnictides, ^[21,22,23,24] the bands having Fe character, as displayed in the middle panel of Fig. 4, show both similarities and remarkable distinctions. Similar to other superconducting Fe pnictides, the d_{yz} and d_{zx} bands lead to electron pockets at the M point. However, instead of three Fe-derived hole pockets at the Γ point, only one Fe d_{zx} -derived hole pocket appears, but this is considerably shrunk in this system compared to other Fe-pnictides (see below). This may imply that the role of Fe for the superconductivity is substantially reduced in this phase.

Most of the Fe bands are separated from the Ti-derived bands, reflecting strong two-dimensionality. Exceptions occur around the M -point and near the Γ point, near E_F . Near the Γ point, the Fe and Ti d_{zx} bands are hybridized with each other, leading to a 0.1 eV gap at E_F . On the other hand, around the M point, the Ti d_{zx} are more strongly hybridized with the Fe d_{zx} and d_{yz} , with the gap of 0.6 eV that occurs above E_F , resulting in surviving M -centered electron pockets. This difference to $\text{Sr}_2\text{VO}_3\text{FeAs}$ results from the different d -orbital filling between V and Ti ions in these systems: namely d^2 for V^{3+} and d^1 for Ti^{3+} .

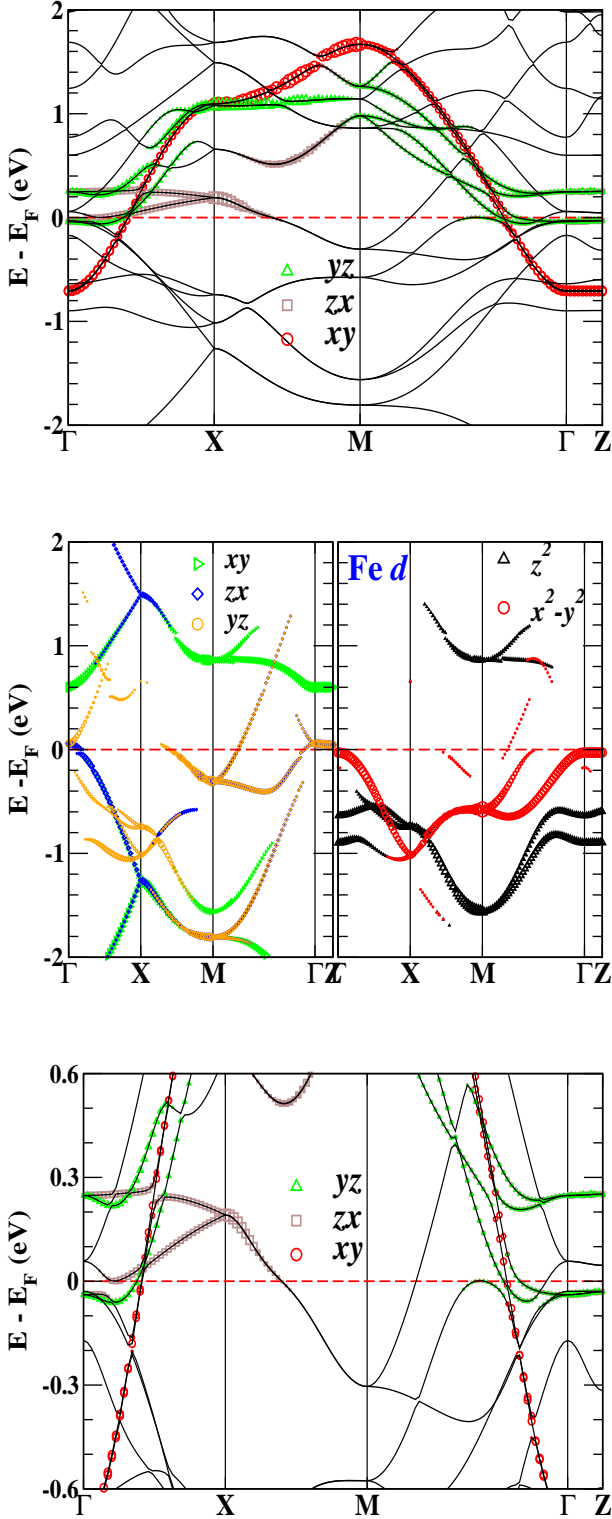


Fig. 4 Top: Band structure, overlapped with the fatband of Ti t_{2g} manifold, on nonmagnetic $\text{Sr}_2\text{TiO}_3\text{FeAs}$. Middle: Fatband representation of Fe d bands. Bottom: Enlarged band structure near E_F with the fatband of Ti t_{2g} manifold, which shows interesting features (see text).

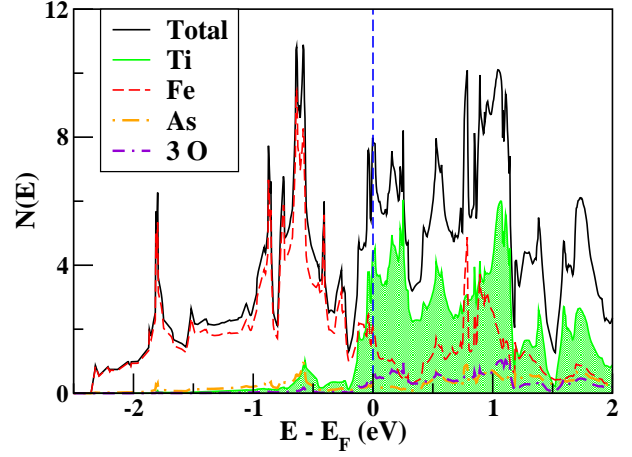


Fig. 5 Total and atom-projected densities of states (DOSs), near E_F , on nonmagnetic $\text{Sr}_2\text{TiO}_3\text{FeAs}$. E_F , denoted by the vertical dashed line, lies on a sharp peak. DOS $N(E_F)$ at E_F is 8.0 states/eV per formula unit: 55% Ti, 25% Fe, and 5% for each O.

As shown in the bottom panel of Fig. 4, noticeable features appear close to E_F . At the Γ point, two-fold bands at -40 meV and 58 meV, and a single band at -30 meV appear. One of the two-fold valence bands is dispersionless near the Γ point along the Γ -X line, leading to a van Hove singularity at -40 meV. On the other hand, one of the doublet conduction bands almost touches with E_F along the Γ -X line, leading to a van Hove singularity almost exactly at E_F . Additionally, one band lying on E_F appears along the M- Γ line (actually a few meV above E_F).

These features are reflected in the total and atom-projected densities of states (emphasized near E_F), given in Fig. 5. A valley appears at -20 meV between the two van Hove singularities at -40 meV and E_F , indicating sensitivity to hole (or electron) doping. This may imply that the stoichiometric sample is near to the optimal doping. $N(E_F)$ is twice as large than for most other Fe pnictides due to the greater contribution of Ti, but is only two thirds of that found in $\text{Sr}_2\text{VO}_3\text{FeAs}$. [7] Remarkably, except for the Ti contribution, the magnitude of $N(E_F)$ is similar with that of LaFeAsO . It is interesting that the T_c of hole-doped LaFeAsO is comparable with the $y = 0.5$ system described herein, in which Ti ions are insulating. This fact suggests that metallic Ti ions can play an important role in the superconductivity of this system.

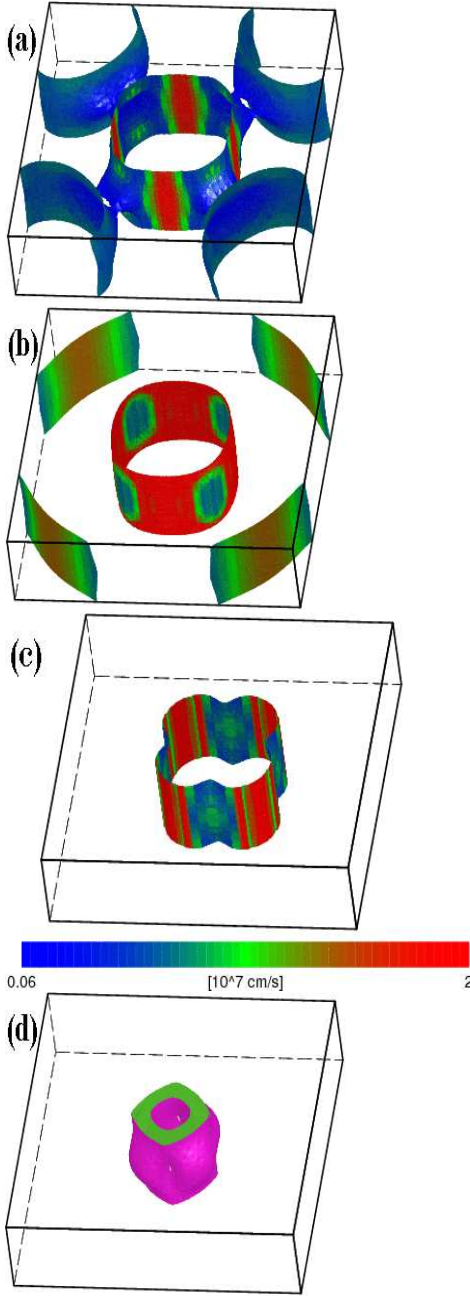


Fig. 6 Fermi surfaces (FSs) of nonmagnetic $\text{Sr}_2\text{TiO}_3\text{FeAs}$. (a)–(c) Fermi velocities v_F colored dark (blue) for the lowest 0.06×10^7 and lighter (red) for the highest 2×10^7 , in units of cm/s. Throughout FS of (d), v_F is remarkably low, $0.6 - 7 \times 10^6$ cm/s. Only (d) and the M -centered FSs have Fe character.

3.3 Fermi surface of nonmagnetic $y=0$ phase

The Fermi surfaces (FSs) consist of five Γ - and two M -centered pockets, as illustrated in Fig. 6. Three large Γ -centered electron pockets have Ti character and the others have Fe character, derived from the d_{zx} band. The character of the M -centered FSs is mostly derived

from the d_{zx} and d_{yz} bands and partially from the $d_{x^2-y^2}$ bands. The M -centered electron pockets possess the shape of an elliptical cylinder (in Fig. 6(a)) and a rhombus (in Fig. 6(b)). In the regime between the two Fe-derived Γ -centered FSs, electrons reside in a coaxial distorted rectangular box-like shape (see Fig. 6(d)). A Fe-derived Γ -centered hole pocket is considered to be a crucial ingredient for the formation of pairings in Fe pnictides, but in this system the pocket is shrunk considerably, implying the opposing view that the metallic Ti ions have a more important role. The three Γ -centered electron pockets are derived from Ti d_{xy} , d_{yz} , and d_{zx} , see Figs. 6(a) to (c). The first two FSs, which are of similar size, are much like MgB_2 .

A large portion of the FSs has remarkably low Fermi velocity v_F , with the lowest being 0.6×10^6 cm/s. In particular, throughout the M -centered elliptical cylinder and the Γ -centered concentric Fe-derived FSs, v_F is close to its lowest value. For the Ti-derived Γ -centered FSs, v_F is quite low along the $\Gamma - M$ line for the two similar sized FSs and along the $\Gamma - X$ line in the remaining FS given in Fig. 6(c).

3.4 Magnetic tendencies of the $y=0$ phase

In this subsection, we will address briefly the possible magnetic tendencies in the Mg-free phase. The competition between superconductivity and magnetic ordering widely observed in Fe pnictides is unclear for this compound, since no magnetic ordering has been observed. Allowing for a ferromagnetic (FM) state, FM has an energy that is a little lower by 5 meV/Fe than for NM. The total magnetic moment is $0.46 \mu_B/\text{Fe}$, mostly comprised of contributions from the Ti ions ($0.37 \mu_B$). The Fe ions are nearly nonmagnetic, less than $0.1 \mu_B$,^[25] suggesting that the magnetic fluctuation due to Ti ions is of more importance than that due to the Fe ions in this phase.

The fixed spin moment (FSM) method was employed to investigate this magnetic behavior, using a cell that allows only FM and NM states. As obtained from LSDA calculations, FSM shows the minimum energy at a total fixed moment of $M=0.45 \mu_B/\text{Fe}$, with an energy 6 meV/Fe lower than in the NM state. From $M=0$ to around the minimum energy state, the Fe moment is quite small and most of the contribution to M results from the Ti moment. After the minimum energy is reached, the moment of Fe increases monotonically, coinciding with a sharp increment in energy with a slope of $\sim 220 \text{ meV}/M$ (M : total moment per formula unit), while that of Ti stays at around $0.6(\pm 0.05) \mu_B$. The Stoner I is 0.47 eV, so $IN(E_F)=2.2$ with $N(E_F)=4.6$

states per eV per formula unit obtained from the FM calculations, indicating strong magnetic instability.

4 Discussion and Summary

For the $y=0$ phase, the on-site Coulomb repulsion U to Ti ions was applied using both popular double-counting schemes in the LDA+U approach,[26,27] to investigate whether or not a Mott transition in the d^1 Ti^{3+} ions occurs. Up to $U=7$ eV $\sim 3W$, which is a much larger value than what has been used in perovskite RTiO_3 (\mathcal{R} =rare earth elements),[28] the Sr_2TiO_3 layers are still metallic. This failure of LDA+U has previously been observed in some $4d$ or $5d$ systems, in which no integer occupation number can occur due to strong p - d hybridization, since an integer occupation is required to lead to a Mott transition by the LDA+U method.[29] In this system, the calculated occupation number is significantly larger than the formal number d^1 , resulting from the absence of rigorous definition of oxidation state in solids, as recently discussed.[30,31] This may prevent the LDA+U approach from driving a Mott transition.[32]

In summary, we addressed the electronic structure of $\text{Sr}_2(\text{Mg}_y\text{Ti}_{1-y})\text{O}_3\text{FeAs}$ for the $y=0.5$ and $y=0$ phases, which represent insulating and metallic Ti layers, respectively. At $y=0.5$, which shows no intrinsic superconductivity, the fermiology is just like that for other Fe-pnictides. Introducing metallic Ti ions, the Γ -centered Fe-derived FSs are reduced considerably or disappeared. Instead, three Γ -centered Ti FSs appear, and two of them have similar sizes like in MgB_2 . Our FSM calculations further suggest possible magnetic ordering in the Ti ions. Although no magnetic ordering has been observed in this compound, the high temperature resistivity measurement shows a kink for samples below $y=0.5$ at $T \sim 200$ K,[13] thus implying magnetic transition. Consequently, a detailed magnetic measurement is required for this compound. Our results indicate that the metallic Ti ions play a crucial role in the superconductivity, suggesting that the mechanism of superconductivity in Fe-pnictides should be reconsidered.

Acknowledgements We acknowledge W. E. Pickett for fruitful communications and H. Ogino for clarifying his experimental results on superconductivity of the $y=0.5$ phase. This research was supported by NRF of Korea under Grant No. 2012-0002245.

References

1. Kamihara, Y., Watanabe, T., Hirano, M., Hosono, H.: Iron-Based Layered Superconductor $\text{La}[\text{O}_{1-x}\text{F}_x]\text{FeAs}$ ($x = 0.05$ -0.12) with $T_c = 26$ K. J. Am. Chem. Soc. **130**, 3296 (2008).
2. Ishida, H., Kakai, Y., Hosono: To what extent iron-pnictide new superconductors have been clarified: A progress report. J. Phys. Soc. Jpn. **78**, 062001 (2009); references therein.
3. Mazin, I.I., Singh, D. J., Johannes, M. D., Du, M. H.: Unconventional Superconductivity with a Sign Reversal in the Order Parameter of $\text{LaFeAsO}_{1-x}\text{F}_x$. Phys. Rev. Lett. **101**, 057003 (2008).
4. Yin, Z. P., Lebegue, S., Han, M. J., Neal, B. P., Savrasov, S. Y., Pickett, W. E.: Electron-Hole Symmetry and Magnetic Coupling in Antiferromagnetic LaFeAsO . Phys. Rev. Lett. **101**, 047001 (2008).
5. Mazin, I.I., Johannes, M. D.: A key role for unusual spin dynamics in ferropnictides. Nature Phys. **5**, 141 (2009).
6. Bang, Y., Choi, H.-Y., Won, H.: Impurity effects on the $\pm s$ -wave state of the iron-based superconductors. Phys. Rev. B **79**, 054529 (2009).
7. Lee, K.-W., Pickett, W. E.: $\text{Sr}_2\text{VO}_3\text{FeAs}$: A Nanolayered Bimetallic Iron Pnictide Superconductor. EPL **89**, 57008 (2010).
8. Arita, R., Ikeda, H.: as compared to other iron-based superconductors Is Fermi-surface nesting the origin of superconductivity in iron pnictides?: A fluctuation-exchange-approximation study. J. Phys. Soc. Jpn. **78**, 113707 (2009).
9. Borisenko, S. V., Zabolotnyy, V. B., Evtushinsky, D. V., Kim, T. K., Morozov, I. V., Yaresko, A. N., Kordyuk, A. A., Behr, G., Vasiliev, A., Follath, R., Büchner, B.: Superconductivity without Nesting in LiFeAs . Phys. Rev. Lett. **105**, 067002 (2010).
10. Qian, T., Wang, X.-P., Jin, W.-C., Zhang, P., Richard, P., Xu, G., Dai, X., Fang, Z., Guo, J.-G., Chen, X.-L., Ding, H.: Absence of a Holelike Fermi Surface for the Iron-Based $\text{K}_{0.8}\text{Fe}_{1.7}\text{Se}_2$ Superconductor Revealed by Angle-Resolved Photoemission Spectroscopy. Phys. Rev. Lett. **106**, 187001 (2011).
11. Ogino, H., Matsumura, Y., Katsura, Y., Ushiyama, K., Horii, S., Kishio, K., Shimoyama, J.: Superconductivity at 17 K in $(\text{Fe}_2\text{P}_2)(\text{Sr}_4\text{Sc}_2\text{O}_6)$: a new superconducting layered pnictide oxide with a thick perovskite oxide layer. Supercond. Sci. Technol. **22**, 075008 (2009).
12. Zhu, X., Han, F., Mu, G., Cheng, P., Shen, B., Zeng, B., Wen, H.-H.: Transition of stoichiometric $\text{Sr}_2\text{VO}_3\text{FeAs}$ to a superconducting state at 37.2 K. Phys. Rev. B **79**, 220512(R) (2009).
13. Sato, S., Ogino, H., Kawaguchi, N., Katsura, Y., Kishio, K., Shimoyama, J., Kotegawa, H., Tou, H.: Superconductivity in a new iron pnictide oxide $(\text{Fe}_2\text{As}_2)(\text{Sr}_4(\text{Mg}, \text{Ti})_2\text{O}_6)$. Supercond. Sci. Technol. **23**, 045001 (2010).
14. Ogino, H., Sato, S., Kishio, K., Shimoyama, J., Tohei, T., Ikuhara, Y.: Homologous series of iron pnictide oxide superconductors $(\text{Fe}_2\text{As}_2)[\text{Ca}_{n+1}(\text{Sc}, \text{Ti})_n\text{O}_y]$ ($n = 3, 4, 5$) with extremely thick blocking layers. Appl. Phys. Lett. **97**, 072506 (2010).
15. Ogino, H., Shimizu, Y., Ushiyama, K., Kawaguchi, N., Kishio, K., Shimoyama, J.: Superconductivity Above 40 K Observed in a New Iron Arsenide Oxide $(\text{Fe}_2\text{As}_2)(\text{Ca}_4(\text{Mg}, \text{Ti})_3\text{O}_y)$. Appl. Phys. Express **3**, 063103 (2010).
16. Ogino, H., Machida, K., Yamamoto, A., Kishio, K., Shimoyama, J., Tohei, T., Ikuhara, Y.: A new homologous series of iron pnictide oxide superconductors $(\text{Fe}_2\text{As}_2)(\text{Ca}_{n+2}(\text{Al}, \text{Ti})_n\text{O}_y)$ ($n = 2, 3, 4$). Supercond. Sci. Technol. **23**, 115005 (2010).

17. Mazin, I.I.: $\text{Sr}_2\text{VO}_3\text{FeAs}$ as compared to other iron-based superconductors. *Phys. Rev. B* **81**, 020507(R) (2010).
18. Lee, C.-H., Iyo, A., Eisaki, H., Kito, H., Fernandez-Diaz, T. M., Ito, T., Kihou, K., Matsuhata, H., Braden, M., Yamada, K.: Effect of Structure Parameters on Superconductivity in Fluorine-Free LnFeAsO_{1-y} ($\text{Ln}=\text{La}, \text{Nd}$). *J. Phys. Soc. Jpn.* **77**, 083704 (2008).
19. Koepnick, K., Eschrig, H.: Full-potential nonorthogonal local-orbital minimum-basis band-structure scheme. *Phys. Rev. B* **59**, 1743 (1999).
20. Schwarz, K., Mohn, P.: Itinerant metamagnetism in YCo_2 . *J. Phys. F:Met. Phys.* **14**, L129 (1984).
21. Singh, D. J., Du, M.-H.: Density Functional Study of $\text{LaFeAsO}_{1-x}\text{F}_x$: A Low Carrier Density Superconductor Near Itinerant Magnetism. *Phys. Rev. Lett.* **100**, 237003 (2008).
22. Lee, K.-W., Pardo, V., Pickett, W. E.: Magnetism driven by anion vacancies in superconducting $\alpha\text{-FeSe}_{1-x}$. *Phys. Rev. B* **78**, 174502 (2008).
23. Lee, K.-W.: Electronic structure of superconducting NaFeAs . *Prog. in Supercond.* **10**, 69 (2009).
24. Mazin, I. I., Johannes, M. D., Boeri, L., Koepnick, K., Singh, D. J.: Problems with reconciling density functional theory calculations with experiment in ferropnictides. *Phys. Rev. B* **78**, 085104 (2008).
25. Using the same internal parameters as in SVOFA[7] and the experimental lattice parameters in this system[13], FM has the large Fe moment of $2.16 \mu_B$, resulting in total moment $2.53 \mu_B$, but much higher energy by ~ 315 meV/f.u. than in the state with nearly nonmagnetic Fe ions which is obtained with our relaxed internal parameters. This fact implies strong magneto-phonon coupling on Fe ions in this system as observed in LaFeAsO . [4]
26. Anisimov, V. I., Zaanen, J., Andersen, O. K.: Band theory and Mott insulators: Hubbard U instead of Stoner I. *Phys. Rev. B* **44**, 943 (1991).
27. Czyzyk, M. T., Sawatzky, G. A.: Local-density functional and on-site correlations: The electronic structure of La_2CuO_4 and LaCuO_3 . *Phys. Rev. B* **49**, 14211 (1994).
28. Pavarini, E., Biermann, S., Poteryaev, A., Lichtenstein, A. I., Georges, A., Andersen, O. K.: Mott transition and suppression of orbital fluctuations in orthorhombic $3d^1$ perovskites. *Phys. Rev. Lett.* **92**, 176403 (2004).
29. Lee, K.-W., Pickett, W. E.: Orbital-quenching-induced magnetism in $\text{Ba}_2\text{NaOsO}_6$. *EPL* **80**, 37008 (2007).
30. Sit, P. H.-L., Car, R., Cohen, M. H., Selloni, A.: Simple, unambiguous theoretical approach to oxidation state determination via first-principles calculations. *Inorg. Chem.* **50**, 10259 (2011).
31. Jiang, L., Levchenko, S. V., Rappe, A. M.: Rigorous definition of oxidation states of ion in solids. *Phys. Rev. Lett.* **108**, 166403 (2012).
32. Pickett, W. E.: private communication.